

TRPC6 is a glomerular slit diaphragm-associated channel required for normal renal function

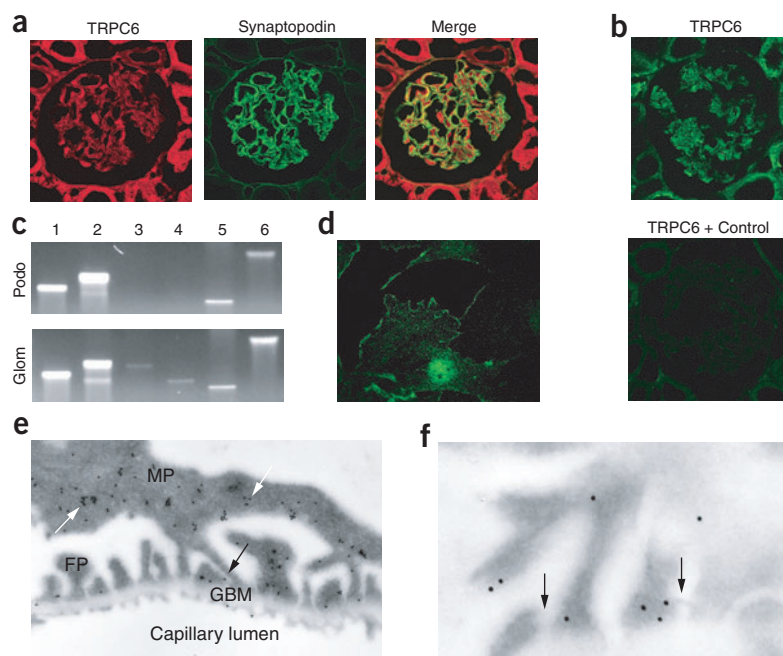
Jochen Reiser¹, Krishna R Polu², Clemens C Möller¹, Peter Kenlan², Mehmet M Altintas¹, Changli Wei¹, Christian Faul³, Stephanie Herbert², Ivan Villegas⁴, Carmen Avila-Casado⁵, Mary McGee⁶, Hikaru Sugimoto⁷, Dennis Brown⁶, Raghu Kalluri⁷, Peter Mundel³, Paula L Smith⁸, David E Clapham⁸ & Martin R Pollak²

Progressive kidney failure is a genetically and clinically heterogeneous group of disorders. Podocyte foot processes and the interposed glomerular slit diaphragm are essential components of the permeability barrier in the kidney. Mutations in genes encoding structural proteins of the podocyte lead to the development of proteinuria, resulting in progressive kidney failure and focal segmental glomerulosclerosis. Here, we show that the canonical transient receptor potential 6 (TRPC6) ion channel is expressed in podocytes and is a component of the glomerular slit diaphragm. We identified five families with

autosomal dominant focal segmental glomerulosclerosis in which disease segregated with mutations in the gene *TRPC6* on chromosome 11q. Two of the *TRPC6* mutants had increased current amplitudes. These data show that TRPC6 channel activity at the slit diaphragm is essential for proper regulation of podocyte structure and function.

Proteinuria is a common feature of kidney dysfunction of glomerular origin and is itself a risk factor for both renal and extrarenal disease¹. The glomerular podocyte is a central component of the renal filtration

Figure 1 TRPC6 expression in the kidney glomerulus. **(a)** Confocal microscopy shows TRPC6 expression (red) in the glomerulus. TRPC6 colocalizes with the podocyte marker synaptopodin (green; overlap shown by yellow staining). **(b)** Compared with the TRPC6 antibody labeling (green), preabsorption of TRPC6 antibody with the control peptide results in negative staining. **(c)** Analysis of *TRPC1–TRPC6* mRNA expression (lanes 1–6, respectively) in cultured podocytes by RT-PCR. *TRPC6*, *TRPC1*, *TRPC2* and *TRPC5* mRNAs are detected in total podocyte RNA (Podo). *TRPC3* and *TRPC4* mRNAs are detected in total glomerular RNA (Glom) but not in total podocyte RNA. **(d)** TRPC6 localizes to the cell membrane in cultured podocytes, as shown by immunostaining (green). **(e)** Immunogold labeling shows TRPC6 localization in podocyte major processes (MP, white arrows) and foot processes (FP). TRPC6 in podocyte foot processes is located in close vicinity to the slit diaphragm (black arrows). GBM, glomerular basement membrane. **(f)** High-power view of slit diaphragm areas (arrows) shows heavy TRPC6 immunogold labeling.



¹Renal Unit, Department of Medicine, Massachusetts General Hospital and Harvard Medical School, Boston, Massachusetts 02129, USA. ²Renal Division, Department of Medicine, Brigham and Women's Hospital and Harvard Medical School, Boston, Massachusetts 02115 USA. ³Department of Medicine, Mount Sinai School of Medicine, New York, New York 10029 USA. ⁴Renal Unit, Instituto del Riñon-Fresenius Medical Care, Colombia. ⁵Department of Pathology, Instituto Nacional de Cardiología Ignacio Chavez, Mexico D.F. 14080, Mexico. ⁶Program in Membrane Biology and Renal Unit, Massachusetts General Hospital and Harvard Medical School, Boston, Massachusetts 02129, USA. ⁷Center for Matrix Biology, Department of Medicine, Beth Israel Deaconess Medical Center and Harvard Medical School, Boston, Massachusetts 02115, USA. ⁸Howard Hughes Medical Institute, Children's Hospital, Department of Cardiology, Boston, Massachusetts 02115, USA. Correspondence should be addressed to J.R. (jreiser@partners.org) or M.R.P. (mpollak@rics.bwh.harvard.edu).

Published online 27 May 2005; doi:10.1038/ng1592

barrier². Podocytes (glomerular visceral epithelial cells) are located in the glomerulus. Their complex cytoarchitecture includes cellular extensions (foot processes) that connect to the glomerular basement membrane on the outer aspect of the glomerular capillaries. Together with the interposed slit diaphragm, a specialized multiprotein junction, they form a crucial component of the ultrafiltration barrier³. This explains why structural damage of the podocyte may lead to the development of proteinuria. Mutations in *ACTN4* (α -actinin-4), *NPHS1* (nephrin) and *NPHS2* (podocin) lead to the development of proteinuric kidney disease⁴. Winn and colleagues identified a family with autosomal dominant focal segmental glomerulosclerosis (FSGS) that segregated with a point mutation in the gene *TRPC6* on chromosome 11q (ref. 5). This prompted us to examine the renal expression and interactions of TRPC6 as well as the spectrum and function of *TRPC6* genetic variants in families with FSGS.

TRPC6 is a member of the transient receptor potential (TRP) superfamily of cation-selective ion channels. The TRPC subfamily (TRPC1–TRPC7) is a group of calcium-permeable cation channels that are important for the increase in intracellular Ca^{2+} concentration after the engagement of G protein-coupled receptors and receptor tyrosine kinases⁶. TRPCs form homo- and heterotetramers that can interact with a variety of other proteins⁷. Because all genes previously described to be mutated in FSGS and nephrotic syndrome are highly expressed in the glomerular podocyte, we examined the expression of TRPC6 in the kidney to define its localization. Confocal microscopy of adult rat kidney sections showed broad expression of TRPC6 throughout the kidney in tubules and glomeruli (Fig. 1a). This observation is consistent with recent reports detecting *TRPC6* mRNA in glomeruli^{5,8}. Most TRPC6 expression in the glomerulus was confined to podocytes (Fig. 1a), as shown by immunofluorescent double labeling with the podocyte marker synaptopodin, resulting in a yellow staining pattern (Fig. 1a)⁹. TRPC6 was also expressed in glomerular endothelial cells.

Figure 3 TRPC6 is upregulated in glomeruli of 2-d-old nephrin-deficient mice, as shown by fluorescence microscopy. Weak TRPC6 expression was detected in glomeruli of 2-d-old wild-type mice (WT; upper panels). TRPC6 was upregulated in glomeruli of 2-d-old nephrin-deficient mice (KO; lower panels). TRPC6 forms aggregates in the glomerulus. Double labeling of TRPC6 with the podocyte marker synaptopodin shows the localization of TRPC6 in kidney podocytes, resulting in yellow staining.

Whereas TRPC6 labeling with the antibody to TRPC6 produced strong glomerular staining and staining in tubules (Fig. 1b), preincubation of TRPC6 antibody with a TRPC6 control peptide resulted in a negative signal (Fig. 1b).

Next, we studied the expression of *TRPC1–TRPC6* mRNAs in isolated glomeruli and cultured mouse podocytes by RT-PCR (Fig. 1c). Whereas *TRPC1–TRPC6* were all expressed in the glomerulus, only *TRPC1*, *TRPC2*, *TRPC5* and *TRPC6* were expressed in cultured podocytes. We analyzed TRPC6 expression in a cultured mouse podocyte cell line¹⁰ and detected labeling at the cell membrane (Fig. 1d). To determine the precise subcellular localization of TRPC6, we carried out immunogold labeling of ultrathin frozen sections from adult kidney cortex (Fig. 1e). Gold particles were found in the cell body of podocytes and in primary processes (Fig. 1e). In podocyte foot processes, gold particles labeled areas in close vicinity to the slit diaphragm region (Fig. 1e). We also detected TRPC6 expression in glomerular endothelial cells (Fig. 1e) and on a few mesangial cells (data not shown). In order for TRPC6 to reach the slit diaphragm in podocyte foot processes, it must be transported from the cell body through the major processes into the foot processes. Membrane proteins with high protein turnover can be found in various subcellular localizations. Similarly, podocalyxin, a major sialoprotein in podocytes, is detected intracellularly throughout the entire exocytotic pathway, consistent with a high rate of synthesis¹¹. High-power

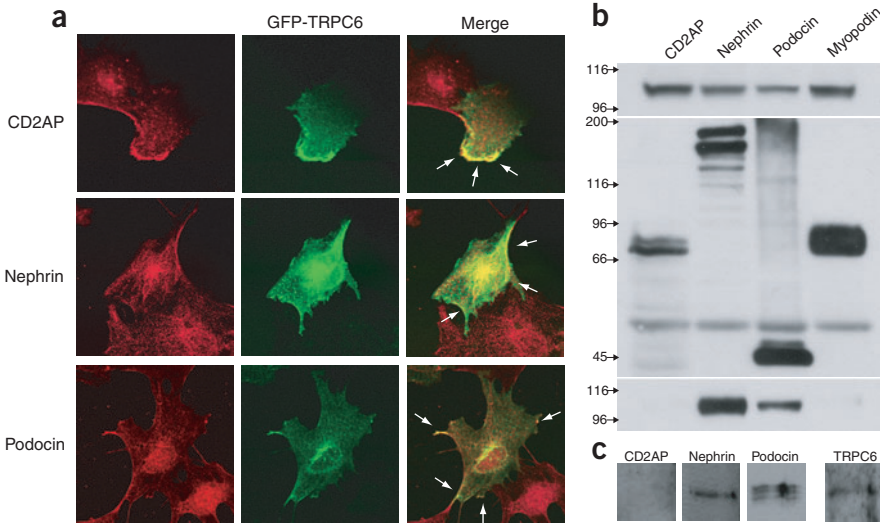
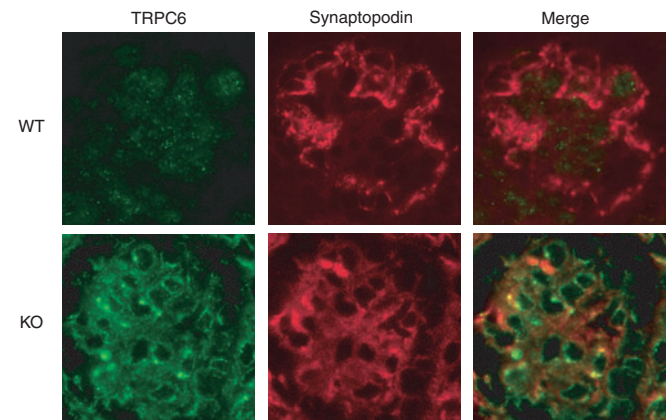


Figure 2 TRPC6 colocalizes and directly interacts with slit diaphragm proteins. (a) GFP-TRPC6 colocalizes with CD2AP, nephrin and podocin at the cell membrane of cultured podocytes, as shown by confocal microscopy (arrows). (b) GFP-TRPC6 associates with FLAG-tagged nephrin and podocin but not CD2AP in cotransfected HEK293 cells. GFP-TRPC6 was detected in total cell lysate by immunoblotting using an antibody to GFP (upper panel). FLAG-tagged fusion proteins were immunoprecipitated, eluted and visualized with an antibody to FLAG (middle panel). Coimmunoprecipitated GFP-TRPC6 was detected in eluate fractions (lower panel). FLAG-myopodin served as a negative control for TRPC6 binding. Apparent molecular weight is shown to the left in kDa. (c) Endogenous coimmunoprecipitation of TRPC6 with slit diaphragm proteins from cultured podocytes. TRPC6 interacts with nephrin and podocin but not with CD2AP. Proteins were immunoprecipitated with antibody to TRPC6.

Table 1 Characteristics of TRPC6 mutations

Family	Ethnicity	Mutation	Exon	Age at disease presentation	Number of family members with ESRD	Change in current amplitude
FG-EA	African American	N143S	2	27–39	5 of 36	No
FG-BN	Colombian	S270T	2	17–52	3 of 12	No
FS-Z	Polish	K874X	12	27–57	9 of 53	No
FG-FQ	Mexican	R895C	13	18–46	6 of 25	Yes
FS-XR	Irish and German	E897K	13	24–35	2 of 12	Yes

Summary of families and TRPC6 variants identified, including range of ages at disease presentation (in y), number of family members known to have end-stage renal disease (ESRD) and indication of whether the variant protein produced an altered current amplitude when expressed in HEK cells. Additional clinical details are given in **Supplementary Note** online.

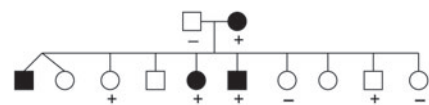
magnification of a section through the slit diaphragm area showed that TRPC6 was closely associated with the slit diaphragm (**Fig. 1f**).

Next, we tested whether TRPC6 colocalizes with the human disease-associated slit diaphragm proteins nephrin, podocin and CD2AP. Because available antibodies against TRPC6 and slit diaphragm proteins are all rabbit polyclonal, we transfected cultured podocytes with green fluorescent protein (GFP)-tagged TRPC6. Confocal microscopy of podocytes transfected with GFP-TRPC6 constructs and stained with antibodies against nephrin, podocin and CD2AP (**Fig. 2a**) showed that GFP-TRPC6 was expressed at the podocyte cell membrane and partially

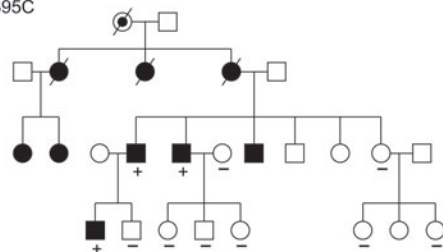
colocalized with endogenous nephrin, podocin and CD2AP^{12–14}. These findings suggest that in podocytes, TRPC6 is at least in part associated with the slit diaphragm.

To test whether TRPC6 interacts with nephrin, podocin or CD2AP, we carried out coimmunoprecipitation studies (**Fig. 2b**). We coexpressed recombinant mouse GFP-TRPC6 with FLAG-tagged mouse nephrin, podocin or CD2AP in human embryonic kidney (HEK293) cells. We immunoprecipitated FLAG fusion proteins from cell lysates using anti-FLAG-M2 beads and analyzed eluates by immunoblotting using antibodies to FLAG and to GFP. To detect the interaction of

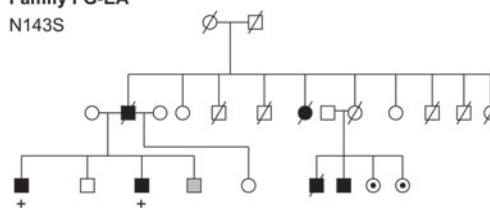
Family FG-BN
S270T



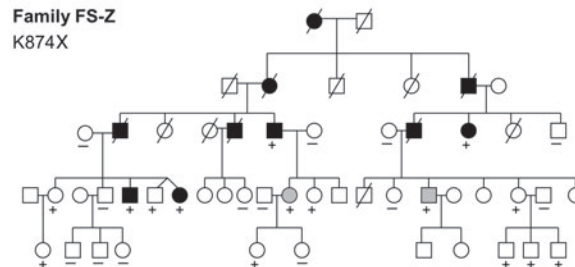
Family FG-FQ
R895C



Family FG-EA
N143S



Family FS-Z
K874X



Family FS-XR
E897K

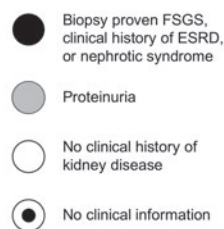
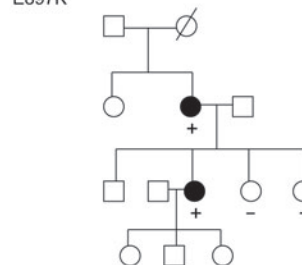


Figure 4 Pedigrees of families with inherited FSGS. *TRPC6* variants segregating in each family are indicated. Genotyped individuals are indicated as carrying (+) or not carrying (–) the variant identified in each family. ESRD, end-stage renal disease.

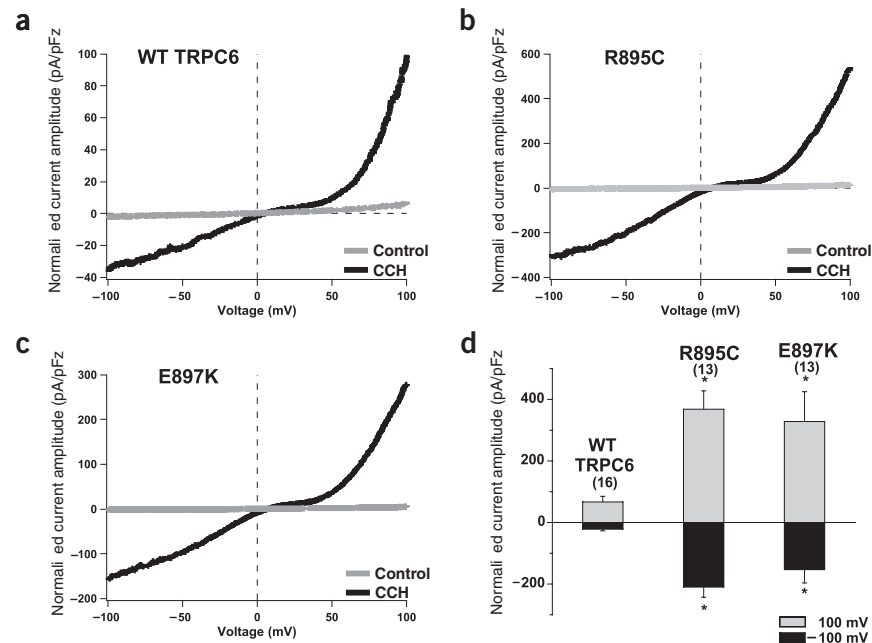


Figure 5 Electrophysiological analysis of mutant TRPC6 channels. Representative whole-cell currents measured from HEK293-M1 cells transiently transfected with cDNA encoding wild-type (WT) TRPC6 (a) or R895C (b) or E897K (c) mutant TRPC6. Current traces were recorded as cells were perfused with control bath solution (gray traces) or 100 μM carbachol (CCh, black traces). Voltage ramps from -100 mV to 100 mV over 150 ms were applied every 3.45 s from a holding potential of 0 mV. Current amplitude was normalized for cell capacitance. (d) Average normalized current amplitude measured at -100 mV (dark bars) and 100 mV (light bars) from cells expressing wild-type (WT) TRPC6 or R895C or E897K mutant TRPC6. Current amplitudes from cells expressing R895C and E897K mutant channels were significantly higher at both -100 mV and 100 mV than those from cells expressing wild-type channels (* $P < 0.01$). The number of experiments for each is shown in parentheses, and the error bars show the s.e.m. for each measurement.

GFP-TRPC6 with FLAG-tagged nephrin, podocin or CD2AP, we analyzed eluates with antibody to GFP. Immunoblotting showed that GFP-TRPC6 was absent from the eluates derived from cells cotransfected with FLAG-CD2AP (Fig. 2b). In contrast, GFP-TRPC6 was present in eluates derived from cells cotransfected with FLAG-nephrin and FLAG-podocin, indicating that TRPC6 had a direct biochemical interaction with nephrin and podocin but not with CD2AP. We also carried out the reverse coimmunoprecipitation, using FLAG-TRPC6 and GFP-tagged slit diaphragm fusion proteins (data not shown). These experiments yielded identical results. We also carried out endogenous coimmunoprecipitation using whole cellular extracts from cultured differentiated podocytes known to express the vital slit diaphragm components nephrin, podocin and CD2AP¹⁵. The immunoprecipitation with antibody to TRPC6 antibody showed that TRPC6 had an interaction with nephrin and podocin but not with CD2AP (Fig. 2c).

Nephrin is a central component of the slit diaphragm, and mice deficient in nephrin suffer from proteinuria and partial foot-process effacement^{16,17}. We therefore examined the effect of nephrin deficiency on the localization of TRPC6 in the glomerulus (Fig. 3). Neonatal wild-type mice had low levels of expression of glomerular TRPC6 (Fig. 3). Some expression was detected in podocytes, as shown by immunofluorescence double labeling with the podocyte marker synaptopodin, resulting in a partial yellow overlap (Fig. 3). The targeted deletion of nephrin led to an induction of podocyte TRPC6 expression and to focal accumulation of TRPC6 (Fig. 3). These data suggest that the lack of nephrin induces podocyte TRPC6 expression and leads to altered cellular localization of TRPC6.

To explore the role of *TRPC6* gene variation in kidney disease, we screened probands of 71 pedigrees with familial FSGS for alterations in *TRPC6* by DNA sequence analysis. Of these 71 families, 43 showed evidence of disease in members of multiple generations, and 28 showed evidence of disease in two or more members of a single generation. Probands of 49% of the families were of western European ancestry; 5% were of African ancestry, and 27% described themselves as Hispanic. The phenotype in affected members of the largest of these families (FS-Z) cosegregated only with chromosome 11q markers (two-point lod score examining linkage of affected individuals with the disease-associated

haplotype equaled 1.8 at $\theta = 0$). We identified different heterozygous sequence variants in five unrelated families with adult-onset disease, all of which predicted changes in the gene product: N143S, S270T, K874X, R895C and E897K (Table 1). We genotyped the relevant variants in other available family members. In all families, *TRPC6* variant and disease inheritance followed a pattern of cosegregation (with less than complete penetrance). In each family, inheritance was consistent with an autosomal dominant pattern (Fig. 4 and Supplementary Note online). Each of the observed amino-acid substitutions occurred in evolutionarily highly conserved residues (Supplementary Fig. 1 online). Two mutations predict amino-acid substitutions in the N-terminal intracellular domain of TRPC6; two predict amino-acid substitutions in the C-terminal intracellular domain; and one encodes a premature stop codon near the C terminus (Supplementary Fig. 1 online). We genotyped 180 control individuals for the disease-associated variants but found none of them. None of these substitutions were found in the public SNP databases either.

To study whether mutations in *TRPC6* affect calcium channel function, we expressed wild-type or one of the five mutant TRPC6 channels in HEK293-M1 cells stably transfected with the $G\alpha_q$ -coupled M1 muscarinic receptor. We recorded TRPC6 currents before and after activation of M1 receptors by carbachol. Currents from N143S, S270T and K874X mutant TRPC6 channels did not differ noticeably from those from wild-type TRPC6 channels (data not shown). In contrast, currents from R895C and E897K mutant channels were significantly larger than those from wild-type TRPC6 channels (Fig. 5). Similarly, Winn and coworkers identified increased current amplitude with the disease-associated TRPC6 P112Q channel⁵. We also noted subtle differences in the rectification of the current-voltage relationship of these two mutants. We believe that these changes in rectification result from the increased current density rather than directly from structure-related changes in channel gating or permeation. If the currents through R895C and E897K mutant TRPC6 channels are similarly increased *in vivo*, these mutations could lead to a gain-of-function alteration in activity and, thus, increased calcium influx.

Three of the *TRPC6* mutations that we identified did not produce apparent changes in current amplitude. Nevertheless, we believe that

these mutations cause disease because of their nature (substitutions in very highly conserved residues or premature stop codon), their cosegregation with the disease phenotype and their absence from control individuals. This suggests that an abnormality other than increased current amplitude is the cause of disease in individuals with these mutations. The several possibilities include altered channel regulation (despite normal amplitude), altered interaction with other slit-diaphragm proteins and altered protein turnover.

Mutations in several podocyte genes have been implicated in susceptibility to progressive renal failure or increased glomerular disease⁴. The presence of *TRPC6* mutations cosegregating with kidney disease; the evolutionary conservation of the altered amino acids, slit-diaphragm localization and interactions; and the gain-of-function changes observed in two mutants suggest that *TRPC6* channel function is essential for normal renal ultrafiltration. The question remains why the onset of kidney disease in individuals with *TRPC6* mutations occurs at a relatively advanced age. Like the adult onset and dominantly inherited form of FSGS caused by mutations of the widely expressed protein α -actinin-4, gain-of-function mutations of *TRPC6* might produce subtle changes in intracellular function that lead to irreversible alterations of cell behavior only after time and in the presence of other renal insults¹⁸. In addition, podocytes express several other TRPC channels, including *TRPC1*, *TRPC2* and *TRPC5* (Fig. 1b). Partial functional redundancy might also account for the late onset of glomerular disease. The ability of *TRPC6* to form heterotetramers with other TRPC channels is suggestive of a complex cellular regulation of calcium homeostasis.

Podocyte electrophysiology has been under investigation for many years¹⁹. Published work has been focused on measurements of the membrane potential and whole-cell conductance in rodent podocytes and their response to vasoactive agonists¹⁹. The location of podocytes within the glomerulus, surrounding the glomerular capillaries, exposes these cells to the transmural hydrostatic pressure driving ultrafiltration. Podocyte foot processes contain a contractile apparatus that may be regulated by slit diaphragm-derived calcium signaling²⁰. Mature podocytes express several types of receptors and second messenger systems³. These include receptors for muscarine, angiotensin, prostaglandin E2 and atrial natriuretic peptide, all of which activate intracellular Ca^{2+} , phospholipase C, inositol 1,4,5-triphosphate, cAMP and cGMP signaling cascades. Thus, podocytes may use foot process- and slit diaphragm-derived intracellular signals to respond to their cellular environment. Nephrin itself is a signaling molecule that generates podocyte survival signals²¹. Fyn kinase is associated with nephrin²² and regulates *TRPC6* channel opening by tyrosine phosphorylation²³. The disruption of nephrin from the slit diaphragm, as has been reported in secondary forms of FSGS²⁴, might mediate its effects on podocytes by modulating *TRPC6*-originated calcium flux. Changes in *TRPC6* calcium currents in podocyte foot processes seem to be central to the ability of the podocyte to regulate its intracellular and cytoskeletal behavior over its lifetime.

METHODS

Immunohistochemistry and immunoelectron microscopy. We perfused female adult Sprague-Dawley rats (body weight = 200 g) through the abdominal aorta with 2% paraformaldehyde in phosphate-buffered saline for 3 min at 220 mm Hg and then with cryoprotectant sucrose-phosphate-buffered saline solution (800 mOsmol) for 5 min at 220 mm Hg. We collected kidneys from wild-type and nephrin-deficient mice, snap-froze them in accordance with standard protocols, sectioned them in ice-cold acetone and then fixed them with 4% formaldehyde. For immunofluorescent labeling, we washed sections once with phosphate-buffered saline and incubated them with blocking solution (2% fetal

calf serum, 2% bovine serum albumin and 0.2% fish gelatin) for 30 min at room temperature before further incubation with the primary antibody for 1 h at room temperature. For double labeling, we applied a second primary antibody for 1 h. We visualized antigen-antibody complexes with secondary antibodies conjugated with fluorochromes. We analyzed specimens using a confocal microscope (Zeiss). We incubated immunogold-labeled ultrathin frozen sections of perfusion-fixed mouse kidney with the rabbit antibody to *TRPC6* (Chemicon) and then with gold-labeled secondary antibody to rabbit. We obtained images using a Philips CM10 electron microscope.

We used the following antibodies: mouse monoclonal antibody G1 to synaptotagmin; rabbit polyclonal antisera to *TRPC6* (Chemicon, Sigma, Alomone 1:50 dilution); and polyclonal antibodies against CD2AP (gift from A. Shaw, Washington University), nephrin and podocin (all at 1:200 dilution). As a negative control, we either omitted the primary antibodies or, in the case of *TRPC6* staining, preincubated the primary antibody with a *TRPC6* control peptide for 1 h before immunolabeling. We analyzed specimens analyzed using a confocal microscope (Zeiss). For immunofluorescent labeling of cultured podocytes, we processed cells as described before¹⁰. We carried out immunofluorescent labeling of nephrin-deficient kidneys as described previously¹⁷.

Coimmunoprecipitation studies. We expressed recombinant mouse GFP-*TRPC6* with FLAG-tagged mouse CD2AP, nephrin or podocin in HEK293 cells. We immunoprecipitated FLAG fusion proteins from cell lysates using anti-FLAG-M2 beads and analyzed eluates by immunoblotting using antibodies to FLAG or to GFP (Sigma).

For endogenous coimmunoprecipitation studies, we prepared whole-cell extracts from cultured differentiated podocytes and incubated them with antibody to *TRPC6* overnight. We then incubated the reaction with protein G-coupled beads (Sigma) for 2 h. We visualized coimmunoprecipitated protein complexes by western blotting using antibodies against *TRPC6* (1:300 dilution), CD2AP (1:2,000), nephrin (1:300) or podocin (1:1,500). As a negative control, we used protein G-coupled beads without antibody.

Cell culture and transfection. We cultured wild-type mouse podocytes as described^{9,25}. The GFP-*TRPC6* construct, which included the complete mouse *TRPC6* cDNA, was provided by M. Zhu (Ohio State University, Columbus, Ohio, USA). We transfected cultured podocytes using standard protocols.

RT-PCR. We isolated total RNA from cultured mouse podocytes using the Trizol reagent (Invitrogen) in accordance with the manufacturer's instructions. We synthesized cDNA using SuperScript II Reverse Transcriptase (Invitrogen) and Oligo(dT)₁₂₋₁₈ oligonucleotide primers in accordance with the manufacturer's instructions.

Clinical recruitment. We obtained blood from members of families with familial FSGS after informed consent was given in accordance with a protocol approved by the Institutional Review Board at Brigham and Women's Hospital. We also obtained clinical history and pedigree information for these families. We measured albumin excretion in urine using a DCA 2000 microalbumin/creatinine analyzer (Bayer). We isolated genomic DNA from peripheral blood leukocytes using Qiagen columns.

Genotyping. We analyzed DNA from probands from 71 families with familial FSGS for mutations in *TRPC6* using bidirectional sequencing. We carried out sequence analysis using PCR-amplified genomic DNA. We used high-throughput capillary sequencing instrumentation and Sanger dideoxy DNA sequencing to detect mutations. Sequence alterations in probands, family members and control subjects were verified using MALDI-TOF mass spectrometry (Sequenom)-based SNP genotyping at the Harvard-Partners Core Genotyping Facility. Primer sequences are given in **Supplementary Table 1** online.

Sequence alignment. We generated sequence alignments using the T-Coffee program comparing human *TRPC6* protein sequences to sequences of other human TRPC channels (*TRPC1* and *TRPC3-TRPC7*) and of *TRPC6* proteins in fly (*Drosophila melanogaster*), rat (*Rattus norvegicus*), mouse (*Mus musculus*), guinea pig (*Cavia porcellus*) and chimpanzee (*Pan troglodytes*)²⁶. We obtained protein sequence data from the National Center for Biotechnology Information database.

Site-directed mutagenesis. We used site-directed mutagenesis to insert the variants identified into a full-length human *TRPC6* cDNA clone (pcDNA3.1-TRPC6). We designed two mutagenic oligonucleotide primers containing the desired mutation and flanked by unmodified nucleotide sequence. We carried out mutagenesis with an amplification reaction using the *TRPC6* cDNA template, mutagenic primers and *Pfu* DNA polymerase. We then selected and sequenced clones to identify and verify mutants.

Electrophysiological analysis of mutant and wild-type TRPC6. We transiently transfected 35-mm dishes of HEK293-M1 cells (human embryonic kidney cells stably transfected with the M1 muscarinic receptor) with 2 μ g of wild-type or mutated *TRPC6* cDNA and 0.25 μ g of eGFP cDNA using Lipofectamine 2000 (Invitrogen). We then plated transfected cells on glass coverslips at low density. We took recordings from cells 24–72 h after transfection. We maintained cells at 37 °C in Dulbecco's modified Eagle medium and Ham's F-12 medium (1:1), 10% fetal bovine serum, 100 U ml⁻¹ penicillin, 100 μ g ml⁻¹ streptomycin and 100 μ g ml⁻¹ G-418 in 5% CO₂.

We visualized eGFP-positive cells with a fluorescence microscope (Olympus) and recorded currents using an Axopatch 200B amplifier and pClamp8 software (Axon Instruments). During voltage ramps, we sampled currents at 10 kHz and filtered the recordings at 2 kHz. In each experiment, we held the membrane potential at either -60 mV or 0 mV (no differences were noted between these experiments). We used borosilicate glass pipettes with resistances of 2–4 M Ω for recording. The bath solution contained 135 mM NaCl, 5 mM CsCl, 2 mM CaCl₂, 1 mM MgCl₂, 10 mM HEPES buffer and 10 mM glucose (pH 7.4). The pipette solution contained 135 mM CsMES, 10 CsCl, 3 mM MgATP, 0.2 mM NaGTP, 0.2 mM EGTA, 0.13 mM CaCl₂ and 10 HEPES buffer (pH 7.3). Free calcium concentration in the pipette solution was ~100 nM as calculated by MaxChelator. We compared average current amplitudes at -100 mV and 100 mV using the Student's *t*-test.

Note: Supplementary information is available on the Nature Genetics website.

ACKNOWLEDGMENTS

We thank the family members for their participation in these studies and M.A. Arnaout for discussions about the manuscript. This work was supported by grants from the US National Institutes of Health (M.R.P., P.M. and R.K.) as well as the Howard Hughes Medical Institute (P.L.S. and D.E.C.). J.R. was supported by the KMD Foundation and the KUFA-ASN Research Grant.

COMPETING INTERESTS STATEMENT

The authors declare that they have no competing financial interests.

Received 12 April; accepted 23 May 2005

Published online at <http://www.nature.com/naturegenetics/>

- Zandi-Nejad, K., Eddy, A.A., Glasscock, R.J. & Brenner, B.M. Why is proteinuria an ominous biomarker of progressive kidney disease? *Kidney Int. Suppl.*, S76–S89 (2004).

- Somlo, S. & Mundel, P. Getting a foothold in nephrotic syndrome. *Nat. Genet.* **24**, 333–335 (2000).
- Pavenstadt, H., Kriz, W. & Kretzler, M. Cell biology of the glomerular podocyte. *Physiol. Rev.* **83**, 253–307 (2003).
- Pollak, M.R. Inherited podocytopathies: FSGS and nephrotic syndrome from a genetic viewpoint. *J. Am. Soc. Nephrol.* **13**, 3016–3023 (2002).
- Winn, M.P. *et al.* A mutation in the TRPC6 cation channel causes familial focal segmental glomerulosclerosis. *Science*, published online 5 May 2005 (doi:10.1126/science.1106215).
- Montell, C. The TRP superfamily of cation channels. *Sci. STKE* **2005**, re3 (2005).
- Clapham, D.E. TRP channels as cellular sensors. *Nature* **426**, 517–524 (2003).
- Facemire, C.S., Mohler, P.J. & Arendshorst, W.J. Expression and relative abundance of short transient receptor potential channels in the rat renal microcirculation. *Am. J. Physiol. Renal Physiol.* **286**, F546–F551 (2004).
- Mundel, P. *et al.* Synaptopodin: an actin-associated protein in telencephalic dendrites and renal podocytes. *J. Cell Biol.* **139**, 193–204 (1997).
- Mundel, P. *et al.* Rearrangements of the cytoskeleton and cell contacts induce process formation during differentiation of conditionally immortalized mouse podocyte cell lines. *Exp. Cell Res.* **236**, 248–258 (1997).
- Schnabel, E., Dekan, G., Miettinen, A. & Farquhar, M.G. Biogenesis of podocalyxin—the major glomerular sialoglycoprotein—in the newborn rat kidney. *Eur. J. Cell Biol.* **48**, 313–326 (1989).
- Boute, N. *et al.* NPHS2, encoding the glomerular protein podocin, is mutated in autosomal recessive steroid-resistant nephrotic syndrome. *Nat. Genet.* **24**, 349–354 (2000).
- Kestila, M. *et al.* Positionally cloned gene for a novel glomerular protein—nephrin—is mutated in congenital nephrotic syndrome. *Mol. Cell* **1**, 575–582 (1998).
- Kim, J.M. *et al.* CD2-associated protein haploinsufficiency is linked to glomerular disease susceptibility. *Science* **300**, 1298–1300 (2003).
- Reiser, J. *et al.* Induction of B7-1 in podocytes is associated with nephrotic syndrome. *J. Clin. Invest.* **113**, 1390–1397 (2004).
- Putala, H., Soininen, R., Kilpelainen, P., Wartiovaara, J. & Tryggvason, K. The murine nephrin gene is specifically expressed in kidney, brain and pancreas: inactivation of the gene leads to massive proteinuria and neonatal death. *Hum. Mol. Genet.* **10**, 1–8 (2001).
- Hamano, Y. *et al.* Determinants of vascular permeability in the kidney glomerulus. *J. Biol. Chem.* **277**, 31154–31162 (2002).
- Kaplan, J.M. *et al.* Mutations in ACTN4, encoding alpha-actinin-4, cause familial focal segmental glomerulosclerosis. *Nat. Genet.* **24**, 251–256 (2000).
- Pavenstadt, H. & Bek, M. Podocyte electrophysiology, *in vivo* and *in vitro*. *Microsc. Res. Tech.* **57**, 224–227 (2002).
- Drenckhahn, D. & Franke, R.P. Ultrastructural organization of contractile and cytoskeletal proteins in glomerular podocytes of chicken, rat, and man. *Lab. Invest.* **59**, 673–682 (1988).
- Huber, T.B. *et al.* Nephrin and CD2AP associate with phosphoinositide 3-OH kinase and stimulate AKT-dependent signaling. *Mol. Cell Biol.* **23**, 4917–4928 (2003).
- Verma, R. *et al.* Fyn binds to and phosphorylates the kidney slit diaphragm component Nephrin. *J. Biol. Chem.* **278**, 20716–20723 (2003).
- Hisatsune, C. *et al.* Regulation of TRPC6 channel activity by tyrosine phosphorylation. *J. Biol. Chem.* **279**, 18887–18894 (2004).
- Bandyopadhyay, B.C. *et al.* Apical localization of a functional TRPC3/TRPC6-Ca²⁺-signaling complex in polarized epithelial cells. Role in apical Ca²⁺ influx. *J. Biol. Chem.* **280**, 12908–12916 (2005).
- Reiser, J., Kriz, W., Kretzler, M. & Mundel, P. The glomerular slit diaphragm is a modified adherens junction. *J. Am. Soc. Nephrol.* **11**, 1–8 (2000).
- Notredame, C., Higgins, D.G. & Heringa, J. T-Coffee: A novel method for fast and accurate multiple sequence alignment. *J. Mol. Biol.* **302**, 205–217 (2000).